

Analysis of high quality superconducting resonators: consequences for TLS properties in amorphous oxides

This content has been downloaded from IOPscience. Please scroll down to see the full text.

2016 Supercond. Sci. Technol. 29 044008

(<http://iopscience.iop.org/0953-2048/29/4/044008>)

View the [table of contents for this issue](#), or go to the [journal homepage](#) for more

Download details:

IP Address: 128.41.61.94

This content was downloaded on 12/04/2016 at 15:32

Please note that [terms and conditions apply](#).

Analysis of high quality superconducting resonators: consequences for TLS properties in amorphous oxides

J Burnett¹, L Faoro^{2,3} and T Lindström⁴

¹ London Centre for Nanotechnology, University College London, 17-19 Gordon Street, WC1H 0AH, UK

² Laboratoire de Physique Théorique et Hautes Energies, CNRS UMR 7589, Universites Paris 6 et 7, 4 place Jussieu, F-75252 Paris, Cedex 05, France

³ Department of Physics and Astronomy, Rutgers The State University of New Jersey, 136 Frelinghuysen Road, Piscataway, NJ 08854, USA

⁴ National Physical Laboratory, Hampton Road, Teddington, TW11 0LW, UK

E-mail: tobias.lindstrom@npl.co.uk

Received 2 December 2015, revised 18 January 2016

Accepted for publication 29 January 2016

Published 11 March 2016



Abstract

1/f noise caused by microscopic two-level systems (TLS) is known to be very detrimental to the performance of superconducting quantum devices but the nature of these TLS is still poorly understood. Recent experiments with superconducting resonators indicates that interaction between TLS in the oxide at the film-substrate interface is not negligible. Here we present data on the loss and 1/f frequency noise from two different Nb resonators with and without Pt capping and discuss what conclusions can be drawn regarding the properties of TLS in amorphous oxides. We also estimate the concentration and dipole moment of the TLS.

Keywords: two level systems, 1/f noise, superconducting device, superconducting resonator, dielectric loss

(Some figures may appear in colour only in the online journal)

1. Introduction

Superconducting electronics has become a frontrunner in the race to create viable applications of solid state quantum technology. For many of these devices superconducting resonators play a fundamental role, both as an integral part of quantum circuits and as a test-bed for developing fabrication technology. Recently, planar on-chip superconducting resonators with internal quality factors Q_i above 10^6 have been developed [1, 2]. The primary challenge in their development has been in the understanding and mitigation of parasitic two-level systems (TLS) which lead to a decrease in Q_i in these resonators at mK temperatures and single photon energies where superconducting qubits are operated [3, 4]. The

presence of TLS is also known to be directly detrimental to coherence times of superconducting qubits.

Despite a large research effort and improvements in quality factors there is as yet no method of completely eliminating parasitic TLS. Instead, the community has found ways of circumventing the problem by using 3D cavities [5]. However, planar devices will almost certainly be necessary in future large-scale integrated quantum circuits meaning the TLS problem will nevertheless have to be solved. Hence, a better understanding of the nature of these TLS is crucial.

Historically, the so-called standard tunnelling model (STM) [6, 7]—first developed to study amorphous glasses in the 1970s—has been used to model the effect of TLS on superconducting resonators. The STM assumes that the TLS have a uniform distribution of the energy splitting and that the interactions between TLS are negligible. Observation of temperature-dependent resonance frequency shifts in high quality resonators agrees with predictions by the STM. However, according to STM theory, one also expects that as



Original content from this work may be used under the terms of the [Creative Commons Attribution 3.0 licence](#). Any further distribution of this work must maintain attribution to the author(s) and the title of the work, journal citation and DOI.

the power of the radiation applied to resonator is increased, the TLS in the dielectrics become saturated, thereby limiting the maximal power that can be dissipated by photons. This results in a strong electric field dependence of the quality factor $Q \propto \sqrt{\langle n \rangle}$, above a critical value n_c . Here $\langle n \rangle \propto \mathcal{E}^2$ is the average number of microwave photons within the superconducting resonator and \mathcal{E} is the electric field applied to the resonator. This power dependence is indeed observed in many resonators characterized by intrinsic loss tangent $\sim 10^{-3}$ at very low powers [3, 8]. However resonators characterized by lower intrinsic loss at low powers typically show much weaker power dependence [4, 9–11]. The failure of the STM to predict the power dependence of the quality factor for the high quality resonators is an indication of a serious gap in our understanding of TLS in amorphous insulators.

It has been suggested [12] that the anomalously weak power dependence can be explained by the assumption that in high-Q superconducting resonators the TLS located at the interfaces are subject to stronger interactions than the TLS located in the bulk dielectrics studied previously. These TLS interactions lead to a drift of the TLS energies that results in a logarithmic dependence of their absorption on the radiation power in agreement with the data.

Further evidence of the importance of TLS interactions was reported in a study of $1/f$ noise in high quality Nb resonator with Pt capping [13]. In that work, data was shown that could not be fit by the conventional STM, instead pointing toward the model in [12] that contains two different types of TLS: ‘slow’ classical fluctuators that can be thermally activated even at millikelvin temperatures with very long time-constants and ‘fast’ coherent TLS with typical energy scales of GHz. Only the latter can directly couple to resonators or qubits, but the two types interact. In particular, the parameters of the coherent TLS are affected by nearby slow fluctuators. This interaction causes the coherent TLS to move in and out of resonance with a microwave resonator or qubit: resulting in a ‘telegraph’-type signal with the familiar $1/f$ noise spectra. It was shown that all features of the low frequency noise in superconducting resonators are captured by this simple model: namely, the frequency dependence of the spectrum $S_y \sim f^{-1}$, the temperature dependence $S_y \sim T^{-B}$ and the applied power dependence $S_y \sim \langle n \rangle^{-1/2}$ as well as the saturation of the noise with the power at the temperature dependent level [13, 14]. More recently, several other groups have published works related to the effects of interacting TLS on resonators and qubits [15–18].

Very recently Burin *et al* [19] argued that interactions between TLS might not be so relevant. They calculated the $1/f$ frequency noise by using the usual STM with the added presence of spectral diffusion and showed that for amorphous solids characterized by ‘typical’ parameters (namely $\chi = 10^{-3}\text{--}10^{-4}$, with $\chi = P_0 U_0$, where P_0 is the typical density of TLS and U_0 denotes the dipole–dipole interaction scale between TLS) in the regime $T < 0.1$ K where the addition of spectral diffusion to the STM predicts an $1/f$ spectrum with $S_y \propto T^{-(1+\mu)}$, where the additional exponent μ is associated with the logarithmic temperature dependence of the spectral diffusion width [20]. Recently Ramanayaka

et al [15] published data that supports this theory in the regime $T < 0.1$ K. However, the experimental data of Burnett *et al* [13], measured at $T \sim \hbar\nu_0/k_B$ where ν_0 is the resonator frequency, cannot be explained by this theoretical result. Burin *et al* [19] therefore argued that the experimental data above 0.1 K might be explained by assuming that, in the high quality resonators the dimensionless parameter, χ is much smaller than typical values in amorphous glasses (for example if the density P_0 or the interaction U_0 between TLS is much smaller than typically expected), also arguing that the relaxation rates of TLS in these resonators can be larger than in ordinary glasses, because of the contribution of conducting electrons in the Pt capping layer.

In an attempt to resolve this controversy we here re-analyse some of our previously published data on a platinum capped Nb lumped element (LE) resonator and supplement it with data on the loss and the $1/f$ frequency noise in a fractal $\lambda/2$ Nb resonator without Pt capping. Prompted by recent experiments by Ramanayaka *et al* [15], we have also studied the ratio between the $1/f$ noise amplitude and the loss tangent.

This paper is organized as follows: we first describe the experimental apparatus and the two different high quality resonators, we then outline briefly the main ideas of our interacting TLS model and recall the formulas for the loss and $1/f$ noise that we derive from the model and we use to fit the data. We present the results and finally discuss implications for the estimates of the parameters characterizing the TLS in these resonators.

2. Experimental

A dilution refrigerator with a base temperature of 50 mK was used for all measurements and the details of this setup have been described in detail elsewhere [3, 13, 21, 22] so only a brief description will be given here. The samples are mounted within a light tight box on a cold stage in contact with the mixing chamber. The box has two microwave lines: one for the input microwave signal which contains 50 dB of attenuation between room temperature and the mixing chamber and room temperature. The second microwave line is for the outgoing microwave signal and contains two microwave 4–8 GHz cryogenic circulators mounted at 700 mK with a HEMT amplifier at 4 K, the noise temperature of this amplifier is ~ 4 K.

Data from two samples are compared in this paper. The first consists of a 50 nm Nb film, with 5 nm Pt capping layer epitaxially grown [23] on a sapphire substrate and patterned into a LE resonator [13] using photolithography and an SF₆/Ar reactive ion etch. The second sample consists of a 200 nm Nb film sputtered onto a sapphire substrate and patterned into a fractal resonator [24] using electron beam lithography and an SF₆/Ar reactive ion etch. An optical micrograph of each resonator can be found in figure 1. Data from both these samples have been previously reported in [13, 25]. A vector network analyser was used to measure the quality factors of the resonators. The resonance has a notch shape and can be described by an equation of the form

$S_{21} = 2 \left[2 + \frac{g}{1 + 2/Q_L x} \right]^{-1}$, where Q_L is the loaded quality factor, g is the coupling parameter and x is the normalized center frequency ($x = (\nu_0 - \nu)/\nu_0$). We note that recent work highlighted the importance of accurate fitting routines and stressed the importance of using notch type resonances to accurately determine the unloaded quality factor Q_u [26]. The *intrinsic* loss tangents $\tan \delta_i$ were determined by measuring the shift of the center frequency as a function of temperature [3] and fitting to the STM. The parameters for the resonators can be found in table 1.

After the initial characterization and measurement of the loss tangent a Pound frequency-locked loop [21] was used to track the frequency jitter in the resonators center frequency [13, 22]. This method allows for high-bandwidth (≈ 10 kHz), high-precision (≈ 1 Hz) direct read-out of the center frequency of the resonator $\nu_0(t)$. For the data presented here, the frequency jitter was measured by fixing the microwave drive and temperature for a period of 1.4 (3) h for the Nb (Nb+Pt) sample. The microwave drive and temperature dependence of the noise is mapped out by repeating the measurement at new combinations of microwave drive and temperature. The fractional frequency spectra S_y (defined as $\langle \delta\nu(t)\delta\nu(t') \rangle / \nu_0^2$) are determined by calculating the overlapping Allan deviation (ADEV) for the jitter time series [27]. This allows for efficient screening of the data since any form of drift that could affect the recorded data over this long time-scales (drifts are readily visible in the ADEV). For time scales $t > 0.01$ s the ADEV reveals a $1/f$ frequency noise characterized by a h_{-1} value. For the $1/f$ noise $S_y = h_{-1}/f$ and we chose a value of 0.1 Hz to analyse the noise in the more familiar form of a power spectral density, $S_y(0.1 \text{ Hz}) = A$.

3. Model

Similarly to the STM, the TLS in our model are described by pseudo-spin operators, S , and are characterized by an uniform distribution of the energy difference, E , between their ground and excited state. In the basis of the eigenstates the Hamiltonian has the simple form $H = ES^z$. The ground and first excited state of the TLS correspond to a quantum superposition of states characterized by different atomic configurations. Each TLS is characterized by a dipole moment $\vec{d}_0 = \vec{d}_0(\sin \theta S^x + \cos \theta S^z)$, which is an operator with both diagonal and off-diagonal components. \vec{d}_0 denotes the difference between the dipole moments in the two different atomic configurations, its magnitude $d_0 = |\vec{d}_0|$ sets the scale of the dipole moment. θ relates the eigenstates of the dipole to a superposition of its states in real space. Because many dipoles have exponentially small amplitude for tunnelling between different positions in real space, the parameters θ and E are assumed to have distribution $\mathcal{P}(E, \theta) dEd\theta \sim P_0/\theta dEd\theta$ for small θ and P_0 .

In the STM the interaction between different TLS is essentially of a dipole–dipole nature with an effective strength given by the dimensionless parameter $\chi = P_0 U_0$ where $U_0 = d_0^2/\epsilon_h$, here ϵ_h is the dielectric constant of the medium

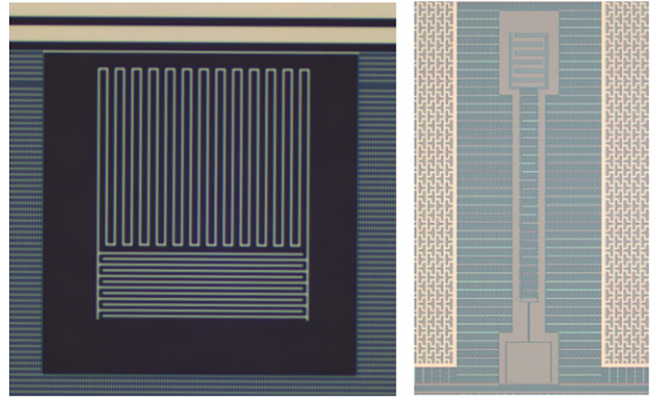


Figure 1. Micrographs of the the two types of resonators used in this work. Left: lumped element resonator. Right: fractal $\lambda/2$ resonator.

Table 1. Device parameters for the resonators used in this work.

Sample	ν_0	Q_L	$Q_u \langle n \rangle \sim 100$
Nb	7.04 GHz	24 000	73 000
Nb+Pt	6.68 GHz	78 000	370 000

Q_L and Q_u denote respectively the loaded and uncoupled quality factor.

that host the TLS. Straightforward analysis shows that the same parameter χ also controls the phonon mean free path at low temperatures [28]. Direct measurements give values of $\chi \approx 10^{-3}\text{--}10^{-4}$ in bulk amorphous materials. We argue that in high quality resonators the TLS located at the interfaces are subject to stronger interactions than the TLS located in the bulk dielectrics. Note that a strong interaction between discrete degrees of freedom always decreases the density of states at low energies, i.e. $\mathcal{P}(E) = P_0(E/E_{\max})^\mu$. For the Coulomb interaction this effect results in a very large suppression of the density of states and the formation of an Efros-Shklovskii pseudogap [29]. The dipole–dipole interaction is small and would result in logarithmic corrections to the density of states for point-like TLS. Because a larger than expected interaction implies that the assumption of point-like defects is probably wrong, we do not in our model attempt to derive the probability distribution $\mathcal{P}(E, \theta)$ in some microscopic picture but instead assume that there is a weak power law dependence of the TLS density of states $\mathcal{P}(E) = P_0(E/E_{\max})^\mu$ with a small parameter $\mu \approx 0.3$ derived from experiments.

The calculation of the noise and the loss in the resonators due to an ensemble of interacting disordered quantum TLS is very difficult. The problem can be simplified if we distinguish between different TLS: coherent or quantum TLS characterized by a dephasing rate $\Gamma_2 < E$ and fluctuators or classical TLS characterized by $\Gamma_2 \geq E$. Among the coherent TLS we distinguish between thermally activated TLS with $E \leq k_B T$ and resonant TLS having an energy splitting $E \approx \hbar\nu_o$, where ν_o is the frequency of the superconducting resonator. We can then calculate how the relevant physical quantities are affected by the interaction between TLS and we find that both the $1/f$ noise and the loss at high fields are strongly affected

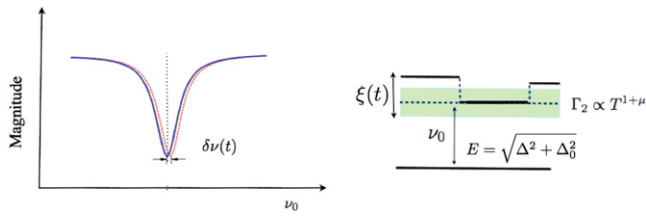


Figure 2. Schematics of the frequency noise generation in microresonators. The noise is due to fluctuators that are strongly coupled to resonant TLS and can induce energy drifts for the resonant TLS larger than the broadening width Γ_2 by bringing the resonant TLS in and out of resonance with the resonator.

by the switching of classical fluctuators that are strongly coupled to resonant TLS. A fluctuator is strongly coupled to a resonant TLS when it is located within a sphere of radius $R_0 = \left(\frac{U_0}{\Gamma_2}\right)^{1/3}$ centred around the resonant TLS. Because the width Γ_2 decreases with temperature, the volume of this sphere will grow as the temperature is lowered. Each fluctuator is described as a random telegraph signal with switching rate γ . Strongly coupled fluctuators induce an energy drift $\xi(t)$ for the resonant TLS larger than the broadening width Γ_2 by bringing the resonant TLS in and out of resonance with the resonator (see figure 2). The drift $\xi(t)$ is a superposition of the random telegraph signals with a distribution of the switching rates $\mathcal{P}(\gamma) = P_\gamma/\gamma$ with normalization constant $P_\gamma = 1/\ln[\gamma_{\max}/\gamma_{\min}]$.

The loss and the frequency noise are related to the average polarization $\mathbf{P}_{\nu_0}(t)$ produced by the resonant TLS:

$$\mathbf{P}_{\nu_0}(t) = \frac{1}{2} \langle \vec{d}_0 \sin \theta \langle S^+(t) \rangle_f \rangle = \varepsilon_h \chi(\nu_0, t) \vec{\mathcal{E}}, \quad (1)$$

where $\langle \cdot \rangle_f$ denotes the average over the distribution of strongly coupled fluctuators responsible for the energy drift and the average $\langle \cdot \rangle$ is taken over the distribution of all the coherent TLS and their dipole moments. Here $\vec{\mathcal{E}}(t) = \vec{\mathcal{E}} \cos \nu_0 t$ is the applied ac electric field.

Specifically, the imaginary part of the average polarization is responsible for the internal quality factor:

$$\frac{1}{Q} = \frac{\int_{V_h} \text{Im}[\mathbf{P}_{\nu_0}(t)] \cdot \vec{\mathcal{E}} dV}{2\varepsilon \int_V |\vec{\mathcal{E}}|^2 dV} \quad (2)$$

and the relative frequency shift is related to the real part of the average polarization:

$$\frac{\delta\nu(t)}{\nu_0} = -\frac{\int_{V_h} \mathcal{Re}[\mathbf{P}_{\nu_0}(t)] \cdot \vec{\mathcal{E}} dV}{2\varepsilon \int_V |\vec{\mathcal{E}}|^2 dV}. \quad (3)$$

The frequency noise spectrum measured in the microresonator is defined as:

$$\frac{S_{\delta\nu}}{\nu_0^2} = \lim_{\tau \rightarrow \infty} \frac{1}{\tau} \int_0^\tau \int_0^\tau \frac{\langle \delta\nu(t_1) \delta\nu(t_2) \rangle}{\nu_0^2} e^{i\omega(t_1-t_2)} dt_1 dt_2. \quad (4)$$

Calculations carried out in [12, 14] show that the interaction with strongly coupled classical fluctuators

(i) results in a formula for the temperature dependent frequency shift that agrees with STM theory:

$$\frac{\delta\nu}{\nu_0} = \frac{F \tan \delta_i}{\pi} \left[\mathcal{Re} \Psi \left(\frac{1}{2} - \frac{\hbar\nu_0}{2j\pi k_B T} \right) - \log \frac{E_{\max}}{2\pi k_B T} \right], \quad (5)$$

(ii) does not change the absorption at low powers but changes the square-root dependence of the absorption into a logarithmic one at high applied fields (we consider the limit of small temperature $\tanh \frac{\hbar\nu_0}{2k_B T} \rightarrow 1$):
— at small field:

$$\frac{1}{Q_i} = F \tan \delta_i \approx F \chi, \quad (6)$$

— at large field:

$$\frac{1}{Q_u(\mathcal{E})} = P_\gamma F \tan \delta_i \ln \left(\frac{\gamma_{\max}}{\Omega} \right), \quad (7)$$

$$\approx P_\gamma F \chi \ln \left(C \frac{|\vec{\mathcal{E}}_{\text{cl}}|}{|\vec{\mathcal{E}}|} \right), \quad (8)$$

where γ_{\max} is the maximum switching rate of the classical fluctuators coupled to the coherent TLS, C is a large constant factor and $\Omega = \frac{|\vec{\mathcal{E}}|}{|\vec{\mathcal{E}}_{\text{cl}}|} \sqrt{\Gamma_1 \Gamma_2}$ denotes the Rabi frequency, \mathcal{E}_{cl} is the critical electric field to saturate the TLS. F is a filling factor which accounts for the fact that the TLS host material volume V_h may only partially fill the resonator volume V :

$$F = \frac{\int_{V_h} \varepsilon_h |\vec{\mathcal{E}}|^2 dV}{2\varepsilon \int_V |\vec{\mathcal{E}}|^2 dV} \approx \frac{1}{2} \frac{\varepsilon_h}{\varepsilon} \frac{V_h}{V}. \quad (9)$$

Note that $\tan \delta_i = \frac{\pi}{3} P_0 \frac{d^2}{\varepsilon_h} \sim \chi$,

(iii) results in a large $1/f$ noise with amplitude:

$$A_0 = \frac{F^2 P_\gamma}{\sqrt{1 + |\vec{\mathcal{E}}|^2 / |\vec{\mathcal{E}}_{\text{cl}}|^2}} \frac{\chi}{N_{\text{TLS}}(T)} \left(\frac{\nu_0}{T} \right)^\mu, \quad (10)$$

Where $N_{\text{TLS}}(T)$ is the number of thermal TLS coupled to the resonator.

4. Results

For both the Nb and Nb+Pt resonators the intrinsic quality factors Q_i were first extracted from measurements of the frequency shifts versus temperature data (this is Q_u in the limit

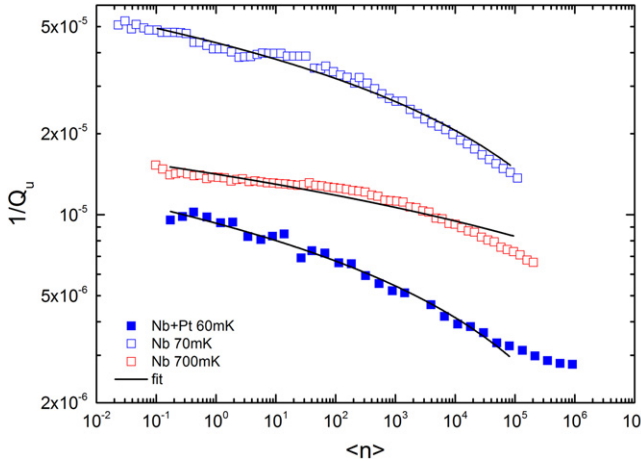


Figure 3. Measurement of the $1/Q_u \propto \tan \delta$. $\langle n \rangle \propto |\vec{E}|^2$ is the average number of microwave photons within the superconducting resonator. Fit with equation (8).

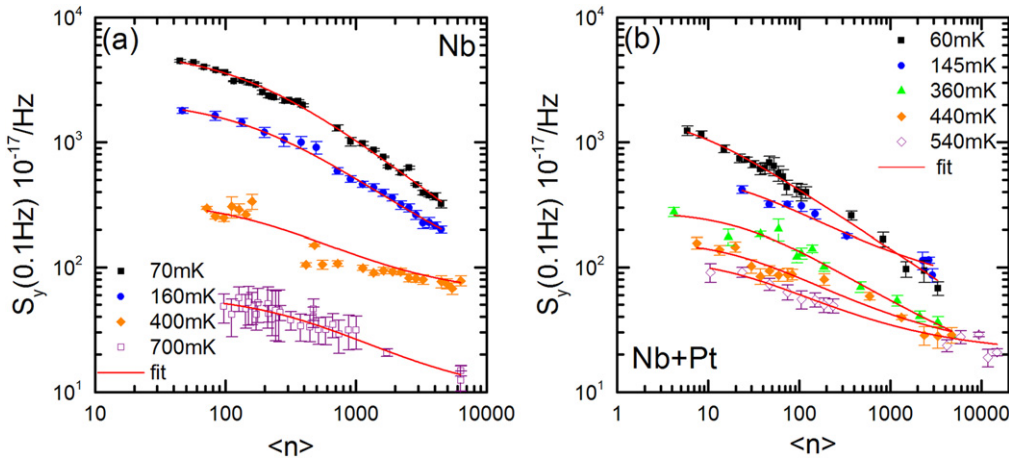
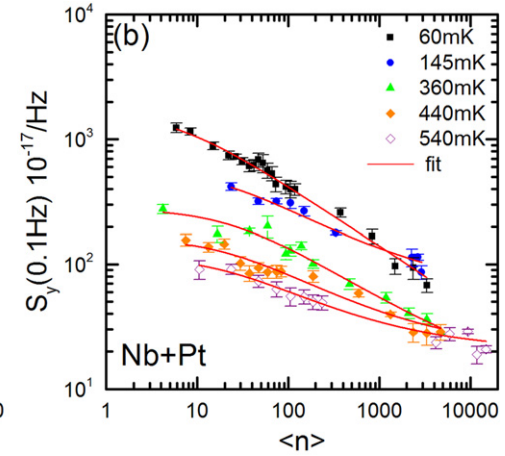


Figure 4. Power spectral density (PSD) of the $1/f$ noise is measured at $S_y(0.1 \text{ Hz})$ in varying temperature and for different average photon energies in the resonator. Shown in red is fit to a power law highlighting an inverse temperature dependence. The noise saturates at a power-dependent level above the system noise floor of $S_y(0.1 \text{ Hz}) = 5 \times 10^{-17}$. The error bars indicate type A uncertainties.

of zero field and zero temperature). Figure 3 shows the power dependent loss $1/Q_u$ which reveals a very weak power dependence that we fit by using the logarithmic formula given in equation (8). We highlight that a fit of the form $Q_u \propto (1 + (\mathcal{E}/\mathcal{E}_c)^2)^\alpha$, finds α to be 0.15 instead of the expected value of 0.5 from the STM. Very low values of α (indicating very weak power dependence of Q_u) was an initial motivator for interacting TLS [12] and justifies our use of equation (8). Data and the prediction of the model are in good agreement. We note that we do not exclude data from any temperature range when fitting to our model, although we are of course aware that the presence of quasiparticles will have an effect for temperatures $T > \hbar\nu_0/k_B$. The fact that a logarithmic dependence is found also for the Nb+Pt resonator implies that the interaction with the conducting electrons present in the Pt capping does not play a role in the relaxation mechanisms of the TLS responsible for the noise. Note that equation (8) is calculated in the low temperature limit; therefore it is unsurprising that the fit is worse for the higher

temperature data in figure 3. The values of the intrinsic quality factors extracted from the frequency shifts versus temperature data and the fits to the loss $1/Q$ are reported in table 2.

Assuming that the TLS are situated in a surface layer $\approx 10 \text{ nm}$ thick, numerical simulations give a filling factor $F \approx 0.01$ for the fractal Nb resonator and $F < 0.01$ for the lumped Nb+Pt resonator. We conclude that in these devices the values of $\chi \approx 10^{-3}$. Notice that we find that the values of the loss tangent estimated from the fit to equation (8) at high fields are smaller than the ones obtained in the measurements of the intrinsic loss tangent at zero fields. This is consistent with our model: in fact, we predict that in the limit of strong applied field the classical fluctuators coupled to resonant TLS cause a drift of the energy splitting and consequently the additional small contribution $P_\gamma = 1/\ln(\gamma_{\max}/\gamma_{\min})$ resulting from averaging over the probability of the switching rates of the classical fluctuators must be taken into account. By



examining the data we find $P_\gamma = 0.1$ for Nb resonator and $P_\gamma = 2 \times 0.1$ for Nb+Pt resonator. Studies of $1/f$ charge noise in single-electron transistor and charge qubits report a spectrum that extends from a few Hertz up to a few MHz [30], implying $\Gamma_{\max}/\Gamma_{\min} \approx 10^4$ and therefore $P_\gamma \approx 1/\ln(10^4) \approx 0.1$. The fact that P_γ is similar for such different resonators provides a further indication that the same mechanism of relaxation are at play in both devices.

Figure 4 shows the microwave drive and temperature dependence of the amplitude A of the $1/f$ frequency spectrum in the two resonators. We note that the larger loss tangent in the Nb sample leads to increased sensitivity to temperature fluctuations (due to permittivity shifts induced by thermal excitation of TLS) and consequently the error bars on this data are larger. Improvements to the measurement setup also made it possible to measure the Nb+Pt resonator at lower microwave drives than the Nb sample. From equation (10) we expect a scaling of the amplitude of the noise with the

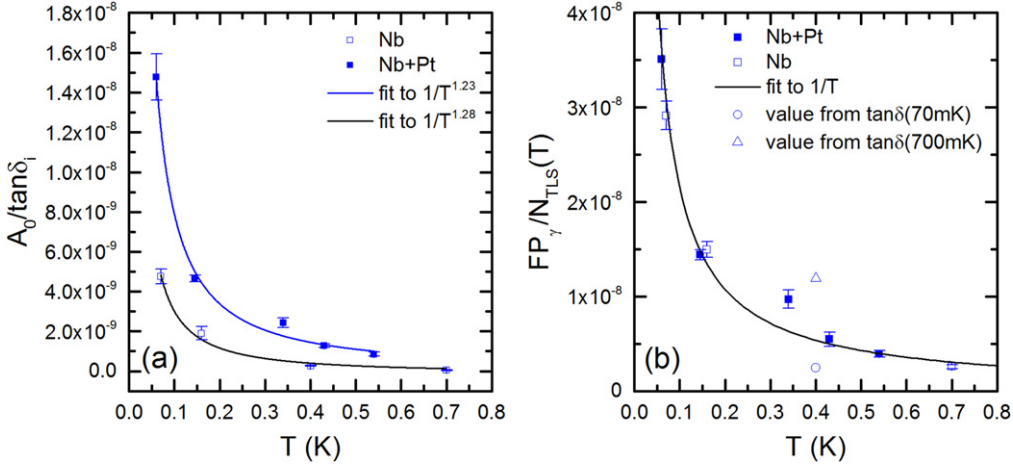


Figure 5. (a) Temperature dependence of the amplitude of the 1/f noise scaled by the loss tangent for the two resonators. The solid lines represent fits to a dependence $T^{-(1+\mu)}$. (b) Temperature dependence of $FP_\gamma / N_{TLS}(T)$ for the two resonators. The solid lines represent fits to a dependence T^{-1} .

microwave drive as $A_0 / \left(1 + \frac{\langle n \rangle}{n_c}\right)^\beta$. We fit our data with $A_0 / \left(1 + \frac{\langle n \rangle}{n_c}\right)^\beta + C$, where $\langle n \rangle \propto \mathcal{E}^2$ is the average number of microwave photons within the superconducting resonator. The values of A_0 and n_c are found to vary with temperature, but we find temperature independent values of β : 0.5 ± 0.05 for the Nb+Pt and 0.75 ± 0.1 for the fractal Nb sample. Hence, whereas the data for the Nb+Pt sample is in good agreement with theory the β -value from the Nb sample does deviate from the expected 0.5, which has also been found in other studies [15]. This could in part be due to that sample mainly having been measured at larger powers where deviations from equation (10) are expected; but could also be due to the design since the electric field distribution in the fractal resonator will be less uniform than in the LE resonator. However, the behavior of both samples is qualitatively the same, despite the design and fabrication process being very different. We note that the model predicts a power independent noise level at low powers due to the desaturation of TLS and another power independent noise level at high powers due to the systematic noise floor. The power independent noise level at low microwave drives is more clearly observed for some low temperatures, but has also been found in other work at very low temperatures [15, 31].

In order to examine how the noise amplitude scales with the loss tangent $\tan \delta_i$ we follow Ramanayaka *et al* [15] and plot the quantity $A_0 / \tan \delta_i$ as a function of temperature in figure 5(a). We find good agreement with equation (10) which predicts a temperature dependence $T^{-(1+\mu)}$ with $\mu = 0.34$ for Nb resonators and $\mu = 0.24$ for the Nb+Pt capping. However, in our resonators we do not find that the scaled quantity $A_0 T / \tan \delta_i$ is T independent as reported in [15].

To give an order of magnitude estimate of the number of thermal TLS that are indirectly coupled to the resonator we examine of the ratio of noise to loss. From equations (10) and (8), we find that in the low field limit the ratio of noise to loss will be $\sim \frac{FP_\gamma}{N_{TLS}(T)} \left(\frac{v_0}{T}\right)^\mu$. Because the last factor can be

estimated using the value of μ found in figure 5(a), this ratio provides information on the number of thermally activated TLS, $N_{TLS}(T)$. The resulting ratio $\sim \frac{FP_\gamma}{N_{TLS}(T)}$ is shown in figure 5(b). To demonstrate the validity, we show a solid line fit to $1/T$, which is the expected dependence since F is a geometric parameter and N_{TLS} is expected to scale as $N_{TLS}(T) = P_0 V_h T$.

We now focus on the Nb+Pt resonator; its lumped nature makes calculations more straightforward. From figure 5(b) we estimate: $N_{TLS}(T) \sim 3 \times 10^4$ at $T = 100$ mK. This is equivalent to an average of ≈ 1 fluctuator μm^{-2} ; comparable to what has been reported for the oxide interface of qubits [32].

Assuming the coherent TLS couple to the resonator via their electric dipole moment the relevant volume is approximately given by the area of the interdigitated capacitor ($100 \times 200 \mu\text{m}^2$) multiplied by the thickness d of the layer, where the TLS are situated; here we will take $d = 10$ nm; giving a total volume of $V_h \approx 2 \times 10^{-10} \text{ cm}^3$. This gives a density of TLS $P_0 = N_{TLS}(T) / V_h T \approx \times 10^{-2} \text{ nm}^{-3} \text{ eV}^{-1}$, that translates into an interaction scale $U_0 = \chi / P_0 \approx 0.1 \text{ eV nm}^3$ for the intrinsic tangent loss $\chi \approx 10^{-3}$ of the oxide. This is significantly larger than the typical values expected for the phonon strain mediated dipole-dipole interaction between TLS in bulk amorphous material, $U_0 \approx 10^{-2} \text{ eV nm}^3$ [20]. The interaction is related to the dipole moment by $U_0 \approx 0.1 \text{ e nm} \approx d_0 / \epsilon_h$. Assuming $\epsilon_h \approx 10$ for the oxide, we get $d_0 \approx 10 \text{ \AA}$. This is a factor $\sim 3\text{--}4$ larger than values reported for conventional glasses, $d_0 = 3 \text{ \AA}$. The reason for this might be a different microscopic origin of TLS in the surface layer; where they could e.g. be due to localized electrons.

Let us now estimate the number of classical fluctuators that are strongly coupled to a resonant TLS. Strongly coupled fluctuators are located within the sphere of radius $R_0 = \left(\frac{U_0}{\Gamma_2}\right)^{1/3}$ from the resonant TLS. In order to calculate their number, we need first to calculate the width Γ_2 of the

Table 2. Experimental parameters used in the calculations.

Sample	ν_0 (GHz)	F_χ	$P_\gamma F_\chi$	$C \vec{\mathcal{E}}_{\text{cl}} (V/m)$
Nb	7.04	$1.2 \pm 0.1 \times 10^{-5}$	$1.22 \pm 0.08 \times 10^{-6}$	3.78×10^7
Nb+Pt	6.68	$1.1 \pm 0.1 \times 10^{-6}$	$2.80 \pm 0.05 \times 10^{-7}$	4.57×10^5

The data in figure 3 is fit to equation (8) to extract the values for $P_\gamma F_\chi$ and $C|\vec{\mathcal{E}}_{\text{cl}}|$, while the values for F_χ are found from a separate measurement of the intrinsic loss tangent. We stress that (8) cannot reliably determine $|\vec{\mathcal{E}}_{\text{cl}}|$ due to the unknown large constant C .

resonant TLS. In the framework of the model [14], the width is: $\Gamma_2 \sim \chi \ln \left(\frac{\Gamma_1^{\max}}{\Gamma_1^{\min}} \right) \frac{T^{1+\mu}}{E_{\max}^\mu}$, where Γ_1^{\max} and Γ_1^{\min} are the maximum and minimum relaxation rate for the coherent TLS and E_{\max} is the maximum TLS level splitting. From spectroscopy of TLS in phase qubits, we estimate $\ln(\Gamma^{\max}/\Gamma^{\min}) \approx 20$, if we assume that the energy splitting extends to chemical energy scales, i.e. $E_{\max} = 100$ K, we find that $\Gamma_2 \approx 2 \times 10^{-5}$ K and the number of strongly coupled fluctuators is $N_f = \frac{4\pi}{3} \frac{\chi T}{\Gamma_2} \approx 20$, which justifies the assumption $N_f \gg 1$ of the model [14].

The data presented in this work and [13] can be well explained by our model. However, we do note that Burin *et al* have suggested an alternative model and has shown [19] that this can be made to fit to data presented for the Nb+Pt sample in [13]; although the fit was restricted to the ($\langle n \rangle \geq 1$) regime and for data taken at $T > 0.1$ K. Equivalent data is not present for the Nb sample making a direct comparison to equation (29) in [19] impossible. Alternatively the data for Nb could be compared to equation (16) in [19] although this comparison is not attempted as it is non trivial. We do note that the fact that a logarithmic power dependence of the loss is seen in both samples implies that the normal electrons in the Pt capping layer in the NP+Pt sample do not play a role in the relaxation.

5. Conclusions

We have analysed the loss and the low frequency $1/f$ noise in two high quality Nb resonator with and without Pt capping and do not find any significant difference in the behavior of the loss and the $1/f$ noise. Both resonators display similar features in the $1/f$ noise spectrum and a weak logarithmic dependent loss $1/Q$ with varying microwave field. We used the model [13] to fit the data and find good agreement. We have also studied the ratio between the noise and the loss and extract order of magnitude estimates for the density of states P_0 , the interaction scale U_0 of the thermally activated TLS in the resonators and the number of classical fluctuators that are strongly coupled to a resonant TLS and in our model are ultimately responsible for the noise and the anomalous weak power dependence of the loss of the resonators at high fields. We find a value of $\chi \approx 10^{-3}$ in agreement with (but somewhat larger) than the values obtained for amorphous glasses; we also find that the interactions scale $U_0 \approx 0.1$ eV nm³ are a factor ~ 10 larger than the typical value of the phonon strain mediated dipole–dipole interaction between TLS expected in amorphous glasses. This interaction energy corresponds to a

dipole moment for the TLS in the oxide layer $d_0 \approx 10$ Å that is again a factor 3–4 larger than expected for TLS in typical amorphous glasses. By comparing the values of the intrinsic quality factors of the resonators extracted from the frequency shifts versus temperature data (limit of zero field and zero temperature) and the ones evaluated from the measurements of Q_i under varying applied microwave powers in the two different resonators, we exclude the presence of additional relaxation due to interaction with conduction electrons in the Pt layer and conclude that the mechanism of the noise in the two different resonators is the same.

Acknowledgments

The authors would like to acknowledge S de Graaf, V L Gurtovoi, R Shaikhaidarov and V Antonov for providing the samples. We would also like to thank S de Graaf, A L Burin, J C Fenton, A Ya Tzalenchuk and L Ioffe for fruitful discussions and comments. This work was supported by the NMS, the EPSRC EP/J017329/1 and by ARO W911NF-13-1-0431.

References

- [1] Megrant A *et al* 2012 Planar superconducting resonators with internal quality factors above one million *Appl. Phys. Lett.* **100** 113510
- [2] Bruno A, de Lange G, Asaad S, van der Enden K, Langford N and DiCarlo L 2015 Reducing intrinsic loss in superconducting resonators by surface treatment and deep etching of silicon substrates *Appl. Phys. Lett.* **106** 182601
- [3] Lindström T, Healey J, Colclough M, Muirhead C and Tzalenchuk A Y 2009 Properties of superconducting planar resonators at millikelvin temperatures *Phys. Rev. B* **80** 132501
- [4] Macha P, van Der Ploeg S, Oelsner G, Ilichev E, Meyer H-G, Wünsch S and Siegel M 2010 Losses in coplanar waveguide resonators at millikelvin temperatures *Appl. Phys. Lett.* **96** 062503
- [5] Paik H *et al* 2011 Observation of high coherence in Josephson junction qubits measured in a three-dimensional circuit qed architecture *Phys. Rev. Lett.* **107** 240501
- [6] Anderson P W, Halperin B and Varma C M 1972 Anomalous low-temperature thermal properties of glasses and spin glasses *Phil. Mag.* **25** 1–9
- [7] Phillips W 1972 Tunneling states in amorphous solids *J. Low Temp. Phys.* **7** 351–60
- [8] Pappas D P, Vissers M R, Wisbey D S, Kline J S and Gao J 2011 Two level system loss in superconducting microwave resonators *IEEE Trans. Appl. Supercond.* **21** 871–4

- [9] Khalil M S, Wellstood F and Osborn K D 2011 Loss dependence on geometry and applied power in superconducting coplanar resonators *IEEE Trans. Appl. Supercond.* **21** 879–82
- [10] Sage J M, Bolkhovsky V, Oliver W D, Turek B and Welander P B 2011 Study of loss in superconducting coplanar waveguide resonators *J. Appl. Phys.* **109** 063915
- [11] Wisbey D S, Gao J, Vissers M R, da Silva F C, Kline J S, Vale L and Pappas D P 2010 Effect of metal/substrate interfaces on radio-frequency loss in superconducting coplanar waveguides *J. Appl. Phys.* **108** 093918
- [12] Faoro L and Ioffe L B 2012 Internal loss of superconducting resonators induced by interacting two-level systems *Phys. Rev. Lett.* **109** 157005
- [13] Burnett J *et al* 2014 Evidence for interacting two-level systems from the $1/f$ noise of a superconducting resonator *Nat. Commun.* **5** 4119
- [14] Faoro L and Ioffe L B 2015 Interacting tunneling model for two-level systems in amorphous materials and its predictions for their dephasing and noise in superconducting microresonators *Phys. Rev. B* **91** 014201
- [15] Ramanayaka A, Sarabi B and Osborn K 2015 Evidence for universal relationship between the measured $1/f$ permittivity noise and loss tangent created by tunneling atoms arXiv:1507.06043
- [16] Lisenfeld J, Grabovskij G J, Müller C, Cole J H, Weiss G and Ustinov A V 2015 Observation of directly interacting coherent two-level systems in an amorphous material *Nat. Commun.* **6** 6182
- [17] Skacel S, Kaiser C, Wuensch S, Rotzinger H, Lukashenko A, Jerger M, Weiss G, Siegel M and Ustinov A 2015 Probing the density of states of two-level tunneling systems in silicon oxide films using superconducting lumped element resonators *Appl. Phys. Lett.* **106** 022603
- [18] Müller C, Lisenfeld J, Shnirman A and Poletto S 2015 Interacting two-level defects as sources of fluctuating high-frequency noise in superconducting circuits *Phys. Rev. B* **92** 035442
- [19] Burin A L, Schechter M and Matityahu S 2015 Low temperature $1/f$ noise in microwave dielectric constant of amorphous dielectrics in josephson qubits *Phys. Rev. B* **92** 174201
- [20] Black J and Halperin B 1977 Spectral diffusion, phonon echoes, and saturation recovery in glasses at low temperatures *Phys. Rev. B* **16** 2879
- [21] Lindström T, Burnett J, Oxborrow M and Tzalenchuk A Y 2011 Pound-locking for characterization of superconducting microresonators *Rev. Sci. Instrum.* **82** 104706
- [22] Burnett J, Lindström T, Oxborrow M, Harada Y, Sekine Y, Meeson P and Tzalenchuk A Y 2013 Slow noise processes in superconducting resonators *Phys. Rev. B* **87** 140501
- [23] Mikhailov G, Malikov I, Chernykh A and Petrashov V 1997 The effect of growth temperature on electrical conductivity and on the structure of thin refractory metal films, grown by laser ablation deposition *Thin Solid Films* **293** 315–9
- [24] de Graaf S E, Danilov A, Adamyan A, Bauch T and Kubatkin S 2012 Magnetic field resilient superconducting fractal resonators for coupling to free spins *J. Appl. Phys.* **112** 123905
- [25] Burnett J, Lindstrom T, Wisby I, de Graaf S, Adamyan A, Danilov A, Kubatkin S, Meeson P J and Tzalenchuk A Y 2013 Pc2: identifying noise processes in superconducting resonators 2013 IEEE 14th International Superconductive Electronics Conference (ISEC) pp 1–3
- [26] Probst S, Song F, Bushev P, Ustinov A and Weides M 2015 Efficient and robust analysis of complex scattering data under noise in microwave resonators *Rev. Sci. Instrum.* **86** 024706
- [27] Rubiola E 2010 *Phase Noise and Frequency Stability in Oscillators (The Cambridge RF and Microwave Engineering Series)* (Cambridge: Cambridge University Press)
- [28] Leggett A J 1991 Amorphous materials at low temperatures: why are they so similar? *Physica B* **169** 322–7
- [29] Efros A and Shklovskii B 1975 Coulomb gap and low temperature conductivity of disordered systems *J. Phys. C: Solid State Phys.* **8** L49
- [30] Kafanov S, Brenning H, Duty T and Delsing P 2008 Charge noise in single-electron transistors and charge qubits may be caused by metallic grains *Phys. Rev.* **78** 125411
- [31] Neill C *et al* 2013 Fluctuations from edge defects in superconducting resonators *Appl. Phys. Lett.* **103** 072601
- [32] Martinis J M *et al* 2005 Decoherence in josephson qubits from dielectric loss *Phys. Rev. Lett.* **95** 210503